

Tunable Majorana corner states in a two-dimensional second-order topological superconductor induced by magnetic fields

Xiaoyu Zhu

School of Science, Xi'an Jiaotong University, Xi'an, Shaanxi 710049, China

(Dated: December 14, 2024)

A two-dimensional second-order topological superconductor exhibits a finite gap in both bulk and edges, with the nontrivial topology manifesting itself through Majorana zero modes localized at the corners, *i.e.*, Majorana corner states. We investigate a time-reversal-invariant topological superconductor in two dimension and demonstrate that an in-plane magnetic field could transform it into a second-order topological superconductor. A detailed analysis reveals that the magnetic field gives rise to mass terms which take distinct values among the edges, and Majorana corner states naturally emerge at the intersection of two adjacent edges with opposite masses. With the rotation of the magnetic field, Majorana corner states localized around the boundary may hop from one corner to a neighboring one and eventually make a full circle around the system when the field rotates by 2π . In the end we briefly discuss physical realizations of this system.

I. INTRODUCTION

Majorana zero modes (MZMs), being mid-gap bound states, are defining features of topological superconductors (TSCs). Just like Majorana fermions[1], a MZM is also the anti-particle of itself, usually denoted by a self-adjoint operator $\gamma = \gamma^\dagger$ [2]. The last decade has witnessed a rapid development in the pursuit of MZMs[3–11], with signatures being reported recently in various systems, such as in nanowire (atomic chain)/superconductor[12–18] or topological insulator/superconductor heterostructure[19, 20], to name a few. Essentially, these systems could realize TSCs under specific circumstances, and MZMs in general emerge at domain walls, for instance, boundaries or vortices, across which the bulk gap of a TSC reverses sign, hence signifying a change of topology.

In contrast to traditional 2D (3D) topological systems where protected gapless modes usually occur on edges (surfaces), very recently it was proposed that topologically nontrivial modes could also emerge at corners (hinges) of certain 2D (3D) systems, coined higher-order topological insulators or superconductors[21–34]. A second-order TSC in 2D, according to the definition, is characterized by Majorana corner states (MCSs), *i.e.*, MZMs bound at corners, where two topologically distinct edges intersect and give rise to a domain wall resembling that in traditional TSCs. Creating such a domain wall at the intersection of neighboring edges is crucial to the realizations of second-order TSCs. To achieve this, one may enforce certain (spatial) symmetries in a traditional TSC at start, as in Ref.[28], where two adjacent edges related by reflection symmetry exhibit gaps of opposite signs, and a symmetry-breaking perturbation weak enough could not immediately eliminate the sign differences and hence the domain wall survives. Alternatively, one could start from a domain wall separating two gapless systems with distinct topology, and apply an external field to gap them out, as was investigated in Ref.[35] on the surface of ${}^3\text{He-B}$, where magnetic field

acting on two gapless domains that are characterized by opposite Ising variables could introduce masses of reverse signs, and therefore a chiral MZM forms at the domain wall.

Up to now, research on second-order TSCs are still at initial stage, with only a few models being put forward to support MCSs[22, 24, 28], and it remains unknown whether these proposals would eventually lead to experimental realizations. In this context, it would be worthwhile to look for other simple as well as physically relevant systems that may support MCSs. In this work, we start from a $p \pm ip$ superconductor, the minimal model of 2D time-reversal invariant TSCs which belong to DIII class[36, 37], and propose that this simple system could support MZMs at its corners when an in-plane magnetic field is applied. We demonstrate that a uniform magnetic field could gap out the edges, whereas edge gaps may reverse signs across certain corners, thus accommodating MZMs inside. By mapping all the four edges to a 1D system, we develop an effective edge theory in which a uniform Zeeman field is projected to a spatially varying mass field, and a single MCS emerges naturally when a kink forms at the intersection of two neighboring edges. In the end, we briefly discuss a more realistic model, Rashba semiconductor/nodeless iron-based superconductor heterostructure in two dimension introduced in Ref.[38], and demonstrate that an in-plane magnetic field could also give rise to MZMs at the corners of this system. Our research may stimulate future searches for MCSs on physical systems that could potentially realize time-reversal-invariant TSCs.

II. MODEL

A $p \pm ip$ superconductor in 2D is characterized by cooper pairing in $p + ip$ form for spin-up (down) electrons and $p - ip$ for spin-down (up) electrons[39]. As such, the superconducting order parameter for the two species differs by a phase π , which is crucial to physical realizations of time-reversal-invariant TSCs. Consider a

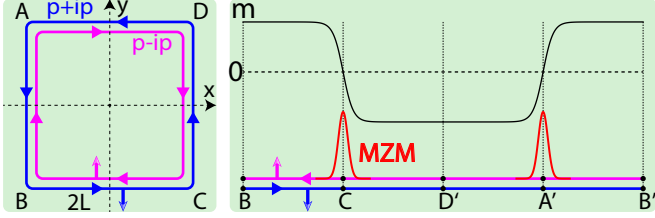


FIG. 1. Left panel. Schematic plot of a 2D $p \pm ip$ superconductor, which features counter-propagating edge modes. Right panel. An effective description of the four edges with a 1D theory. In presence of an in-plane Zeeman field, the mass gap m induced varies across edges and MZMs emerge at corners where m reverses sign and forms a kink.

$2L \times 2L$ square lattice for such a system when subject to an in-plane magnetic field, with tight binding Hamiltonian given by

$$H = -t \sum_{\langle \mathbf{r} \mathbf{r}' \rangle \alpha} c_{\mathbf{r} \alpha}^\dagger c_{\mathbf{r}' \alpha} + \sum_{\mathbf{r} \alpha \alpha'} c_{\mathbf{r} \alpha}^\dagger (\mu \sigma_0 + \mathbf{V} \cdot \boldsymbol{\sigma})_{\alpha \alpha'} c_{\mathbf{r} \alpha'} + \frac{\Delta}{2} \sum_{\mathbf{r} \alpha} e^{is_\alpha \phi} (c_{\mathbf{r} \alpha}^\dagger c_{\mathbf{r} + \hat{\mathbf{e}}_y, \alpha}^\dagger - is_\alpha c_{\mathbf{r} \alpha}^\dagger c_{\mathbf{r} + \hat{\mathbf{e}}_x, \alpha}^\dagger) + \text{H.c.}, \quad (1)$$

where t terms include only nearest-neighboring hopping, μ denotes chemical potential, $\mathbf{V} = (V_x, V_y, 0)$ represents the Zeeman field induced by an external magnetic field in the plane, $\hat{\mathbf{e}}_x$ and $\hat{\mathbf{e}}_y$ denote unit vectors along x and y directions, $\boldsymbol{\sigma}$ represent Pauli matrices, σ_0 stands for identity matrix, and α refers to spin indices with $s_\uparrow = 1$ and $s_\downarrow = -1$. In this model, spin-up and spin-down electrons condense into cooper pairs of $p - ip$ and $p + ip$ form separately, with pairing strength Δ being the same for both and the global superconducting phase ϕ taking opposite signs as is guaranteed by time reversal symmetry (TRS).

Imposing periodic boundary conditions (PBCs) in both directions, we could obtain the momentum representation of lattice Hamiltonian (1), which takes the form

$$H = \frac{1}{2} \sum_{\mathbf{k}} \Psi_{\mathbf{k}}^\dagger \mathcal{H}(\mathbf{k}) \Psi_{\mathbf{k}} \quad (2)$$

$$\mathcal{H}(\mathbf{k}) = \epsilon(\mathbf{k}) \tau_z - \Delta \tau_x (\sin k_x \sigma_x - \sin k_y \sigma_y) + \tilde{\mathbf{V}} \cdot \boldsymbol{\sigma},$$

where τ_i and σ_i ($i = x, y, z$) are Pauli matrices acting in particle-hole and spin space respectively, the Nambu spinor $\Psi_{\mathbf{k}} = e^{-i\frac{\phi}{2}\sigma_z} \{c_{\mathbf{k}\uparrow}, c_{\mathbf{k}\downarrow}, c_{-\mathbf{k}\downarrow}^\dagger, -c_{-\mathbf{k}\uparrow}^\dagger\}^T$ (note the prefactor is added to eliminate the phase ϕ in superconducting terms), kinetic energy $\epsilon(\mathbf{k}) = \mu - 2t(\cos k_x + \cos k_y)$, and the effective Zeeman field $\tilde{\mathbf{V}} = (V \cos(\theta + \phi), V \sin(\theta + \phi), 0)$, with $\theta = \arg(V_x + iV_y)$.

In absence of Zeeman fields, the system preserves time reversal symmetry $\mathcal{T} = i\sigma_y \mathcal{K}$ (\mathcal{K} denotes conjugation operator), particle-hole symmetry $\mathcal{P} = \tau_y \sigma_y \mathcal{K}$, and in addition C_4 rotation symmetry given by

$$\mathcal{U}_R \mathcal{H}(\mathcal{R}^{-1} \mathbf{k}) \mathcal{U}_R^{-1} = \mathcal{H}(\mathbf{k}), \quad (3)$$

with the unitary transformation $\mathcal{U}_R = e^{-i\frac{\pi}{4}\sigma_z}$, and $\mathcal{R}(k_x, k_y) = (k_y, -k_x)$. Turning on a finite Zeeman field breaks TRS and C_4 rotation symmetry, but one can in this circumstance define an inversion symmetry \mathcal{I} up to a gauge transformation, which reads

$$\mathcal{U}_I \mathcal{H}(\mathcal{I}^{-1} \mathbf{k}) \mathcal{U}_I^{-1} = \mathcal{H}(\mathbf{k}), \quad (4)$$

with $\mathcal{U}_I = \tau_z$ and $\mathcal{I}\mathbf{k} = -\mathbf{k}$. The bulk spectrum is supposed to preserve this inversion symmetry, and takes the following form

$$E(\mathbf{k}) = \pm \sqrt{(\sqrt{\epsilon^2(\mathbf{k}) + \Delta_-^2(\mathbf{k})} \pm V)^2 + \Delta_+^2(\mathbf{k})}, \quad (5)$$

with $\Delta_-(\mathbf{k}) = \Delta[\cos(\theta + \phi) \sin k_x - \sin(\theta + \phi) \sin k_y]$, and $\Delta_+(\mathbf{k}) = \Delta[\sin(\theta + \phi) \sin k_x + \cos(\theta + \phi) \sin k_y]$. The model in absence of Zeeman fields admits gapless modes only when μ is fine tuned to 0 or $\pm 4t$. Away from these phase transition points when $\mu \in (-4t, 0) \cup (0, 4t)$, the system is fully gapped and resides in topologically non-trivial phases, in the sense that it cannot be smoothly connected to the vacuum and hence gapless modes would emerge at each edge, as illustrated in the left panel of Fig. 1. Zeeman fields may gap out the edge modes and meanwhile reduce the gap size at Brillouin zone center $\Gamma(0, 0)$, corners $M(\pi, \pi)$ and centers of edges $X(0/\pi, \pi/0)$, as can be seen in Eq.(5). A strong field, however, would drive the system into a nodal superconductor, with nodal points appearing in pairs due to inversion symmetry. In this work, we mainly work in the regime where the Zeeman field is weak enough such that the bulk gap in topologically nontrivial phases is always finite. This way one could focus on the edges, which we shall investigate in the following.

III. EDGE HAMILTONIAN

As a first step, let us turn off the Zeeman field for the moment and then write down wave functions of MZMs on each edge following the procedure outlined in Ref.[40], which are given by

$$\Psi_{\alpha}^{\text{Edge}}(r) = \mathcal{A} \psi_{\alpha}^{\text{Edge}} [e^{\lambda_+(\delta r - L)} - e^{\lambda_-(\delta r - L)}], \quad (6)$$

where the spinors $\psi_{\uparrow}^{\text{Edge}} = \{-e^{i\varphi_n}, 0, 0, e^{-i\varphi_n}\}$, $\psi_{\downarrow}^{\text{Edge}} = \{0, e^{-i\varphi_n}, e^{i\varphi_n}, 0\}$, with $\varphi_n = \frac{n}{4}\pi$, and \mathcal{A} is the normalization constant. Without loss of generality, t and Δ are assumed to be positive and λ_{\pm} , being the reverse of decay length, are given by the two roots of characteristic equation $t\lambda^2 - \Delta\lambda - \mu + 4t = 0$. Variables n, δ, r appearing in Eq.(6) take different values depending on the edge considered and are listed in the following table.

Edge	AB	BC	CD	DA
n	1	2	3	4
r	x	y	x	y
δ	—	—	+	+
ν	+	—	—	+

We note that, in deriving Eq.(6) $\mu \lesssim 4t$ is assumed, in which case we could have $\cos k_r \approx 1 - \frac{1}{2}k_r^2$ and $\sin k_r \approx k_r$, with $r = x, y$, around Γ point. Similarly, one may consider the case when μ is close to the other two phase transition points, and in those circumstances expand sine and cosine terms around M or X points, which would lead to the same results except that the wave functions for edge modes may acquire additional oscillating terms like $e^{i\pi r}$. Clearly MZMs in Eq.(6) always come in pairs, one for each spin. Upon projecting the bulk Hamiltonian (2) onto edge space spanned by the basis $\{\Psi_{\uparrow}^{Edge}(r), \Psi_{\downarrow}^{Edge}(r)\}^T$ for a given edge, one could then obtain corresponding edge Hamiltonian, which reads

$$\mathcal{H}^{Edge}(k_{\bar{r}}) = \nu \Delta k_{\bar{r}} \eta_z - V \sin(\theta + \phi + 2\varphi_n) \eta_y, \quad (7)$$

where η_i are Pauli matrices acting in edge space, ν for each edge is listed in the table above, $\bar{r} = x$ if $r = y$ and vice versa. In Eq.(7), the kinetic term proportional to Δ exactly describes two Majorana modes propagating in opposite directions, whereas the η_y term originating from the Zeeman field couples the two modes, thus opening a finite edge gap. Interestingly, the gap induced by the same Zeeman field differs among the four edges. This is because for each edge only certain component of the Zeeman field could be projected onto the edge space. To make it concrete, let us take Edge BC and CD , shown in the left panel of Fig. 1, as two examples for comparison. First, as one can verify, $\tau_y \sigma_y \psi_{\alpha}^{BC} = -\psi_{\alpha}^{BC}$. When the bulk Hamiltonian was projected onto the edge space spanned by the basis $\{\Psi_{\uparrow}^{BC}, \Psi_{\downarrow}^{BC}\}^T$, those terms anti-commuting with $\tau_y \sigma_y$ would be projected out. Hence $V \cos(\theta + \phi) \sigma_x$ in Eq.(2) wouldn't appear in the edge Hamiltonian. Similarly, $V \sin(\theta + \phi) \sigma_y$ would be projected out on Edge CD , since $\tau_y \sigma_x \psi_{\alpha}^{CD} = -\psi_{\alpha}^{CD}$ and σ_y anti-commutes with $\tau_y \sigma_x$. So we establish that for a given Zeeman field applied, each edge only feels part of it, which differs from one another.

IV. MAJORANA CORNER STATES

So far, we have only considered PBCs, imposed either in one or both directions, corresponding to a system being put on a cylinder or torus. Now we turn to a finite lattice with free boundaries in both directions, in which case the four edges are all well defined. One can expect that the spectrum of edge modes determined by Hamiltonian (7) could still be valid at least qualitatively. Indeed, as shown in Fig.2(a), the edge gap for a finite lattice agrees well with theoretical values— minimum of the four edge gaps— given by Eq.(7). Due to the fact that each edge only feels part of the Zeeman field, edge-gap size oscillates with the orientation θ of the Zeeman field, with period of oscillation being $\frac{\pi}{2}$. In addition, we find that two MZMs (only one was shown in Fig. 2) always exist, even when certain edges become gapless, corresponding to θ being an integer multiple of $\frac{\pi}{2}$. A further investigation reveals that the two MZMs are bound at corners

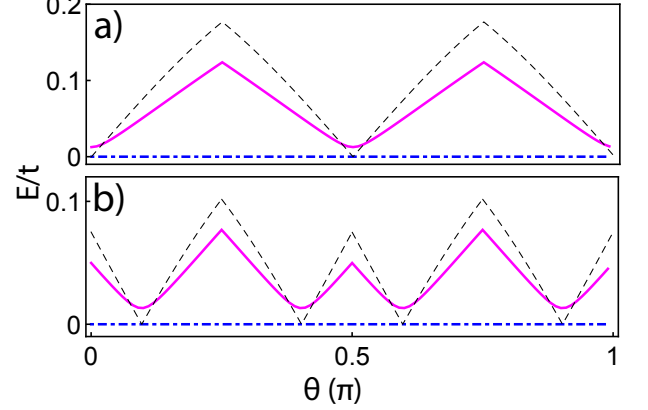


FIG. 2. Variations of the edge gap with the orientation θ of the Zeeman field for a 80×80 lattice. Blue (dot dashed) line represents one of the two zero modes, magenta (solid) line reflects the edge gap, and black (dashed) line are edge gaps determined by the minimum of mass terms in Eq.(7) for the four edges. $t = 1$, $\mu = 3$, $\Delta = 1$, $\phi = 0$ and $V = 0.5$. Panel b) $\Delta_s = -0.15$.

on the same diagonal, as can be seen from the probability density plot in Fig.3 (a)-(d). While the Zeeman field rotates in the plane, these MCSs may hop from one corner to another, and in some special cases reside on certain edges, which is due to the vanishing of mass terms on these edges. When the Zeeman field rotates by 2π , each MCS would complete one revolution around the lattice and return to its original position. To figure out when and where (which corners) these MZMs could form, we need to identify the relative signs of mass terms among the four edges. However, we should note that, the mass terms appearing in Eq.(7) couldn't be applied straightforwardly since the edge Hamiltonian was written in different basis for each edge. Therefore, we may consider to express them in the same edge basis, in which case the four edges actually form a 1D system, provided the bulk gap is sufficiently large such that edges on opposite sides have negligible overlap. In the following, we shall develop an effective theory to describe these edges in a unifying frame, based on the edge Hamiltonian already obtained.

We first note that, without Zeeman fields edge modes in a finite lattice are supposed to circle around all the four edges due to C_4 rotation symmetry defined in Eq.(3). The same symmetry requires that spinors ψ_{α}^{Edge} in Eq.(6) for an edge mode flowing on the four edges are connected by unitary transformation \mathcal{U}_R , to be specific,

$$\psi_{\alpha}^{AB} = \mathcal{U}_R \psi_{\alpha}^{BC} = \mathcal{U}_R^2 \psi_{\alpha}^{CD} = \mathcal{U}_R^3 \psi_{\alpha}^{DA}. \quad (8)$$

Since $\mathcal{U}_R^4 = -1$, ψ_{α}^{Edge} would acquire a minus sign after the mode makes a full circle, in contradiction with single-valuedness of wave functions. Hence there has to be another term in the wave function that also contributes to a minus sign. Notice that for an edge mode with finite energy E , the wave function Ψ_{α}^{Edge} in Eq.(6) needs to

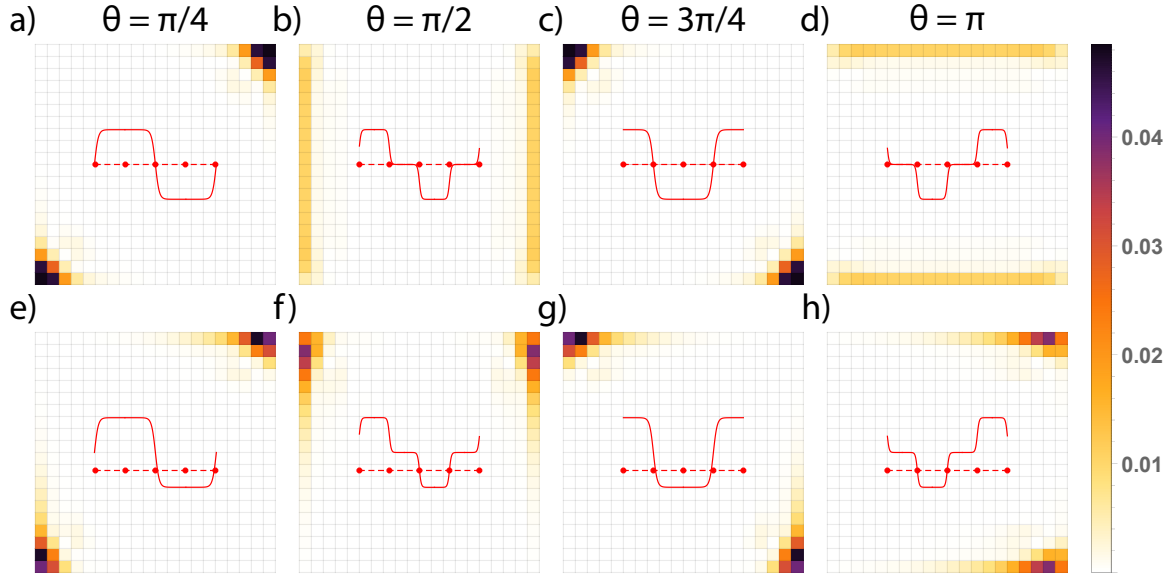


FIG. 3. Probability density distribution of MZMs for a 20×20 lattice. Insets are the mass profile on 1D system shown in the right panel of Fig.1, with dotted line representing zero masses and red dots denoting the corners. $t = 1$, $\mu = 3$, $\Delta = 1$, $\phi = 0$ and $V = 0.5$. For (e)-(h) $\Delta_s = -0.15$.

be modified by multiplying an oscillating term e^{ikr} with $k = \frac{2E}{\Delta}$ (the prefactor 2 originates from $\frac{1}{2}$ in Hamiltonian (2)). To produce a minus sign, we then expect kr to increase or decrease by an odd multiple of π when an edge mode goes back to its original position after a complete revolution, *i.e.*, $kP = (2n + 1)\pi$ with P being perimeter of the lattice. Therefore no gapless modes would exist in a finite lattice. This resembles the spinless $p + ip$ TSC on an annulus in Ref.[8], where edges modes flowing on the inner and outer edges are also gapped, and the infinite-order rotation symmetry of annulus requires the spinor part to rotate all the way while the gapped edge modes flow. In Fig.4, we plotted the phase evolution on

the boundary sites for each component of the two lowest positive edge modes, one for each spin, with wave functions denoted by $\{u_\uparrow, v_\uparrow\}$ and $\{u_\downarrow, v_\downarrow\}$ respectively. As is demonstrated in Fig.4, the phase experiences an abrupt change around each corner, corresponding to the rotation of spinor part, in agreements with Eq.(8). Instead, on the edges the phase varies smoothly, which is due to the spatially oscillating term. Clearly, for a mode with positive energy spin-up modes propagate clockwise whereas spin-down modes propagate counterclockwise, both characterized by a constant modulus of wave vector, being $k = \frac{\pi}{P}$, which can be readily evaluated from the slope of phase curves on each edge shown in Fig.4.

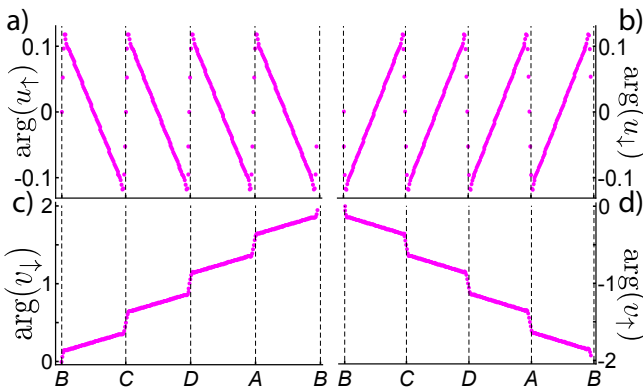


FIG. 4. Phase for edge modes with lowest positive energy along the boundary sites of a 80×80 lattice. The phase for each component is given by its argument relative to that of site B . The values shown on vertical axis are expressed in unit of π . $t = 1$, $\mu = 3$, $\Delta = 1$, $\phi = 0$ and $V = 0.5$.

The fact that C_4 rotation occurs abruptly around the corners and that edge modes behave in a similar fashion on each edge motivates us to develop a 1D theory to describe the four edges effectively. Since the modes on adjacent edges are related to each other through Eq.(8), we may rotate them into the same form. In practice, we fix Edge BC and map the other three edges onto the direction of BC as shown in right panel of Fig. 1. As a result the four edges are linked together in a 1D system and edge modes flowing in this 1D system share the same spinor part. This transformation actually amounts to reversing the rotation each edge mode experiences at the corners and letting the mode flow instead along the original direction, say from Edge BC to CD' rather than CD . As a result, no rotations, either in real space or spinor space would occur while edge modes move across each corner. Along with the rotation of wave functions for individual edges, the bulk Hamiltonian should be rotated accordingly in order to preserve the energy spectrum, with the specific form in momentum representation

given by

$$\begin{aligned} CD \rightarrow CD' : \quad & \mathcal{H}'(\mathbf{k}) = \mathcal{U}\mathcal{H}(\mathcal{R}^{-1}\mathbf{k})\mathcal{U}^{-1} \\ DA \rightarrow D'A' : \quad & \mathcal{H}'(\mathbf{k}) = \mathcal{U}^2\mathcal{H}(\mathcal{R}^{-2}\mathbf{k})\mathcal{U}^{-2} \\ AB \rightarrow A'B' : \quad & \mathcal{H}'(\mathbf{k}) = \mathcal{U}^{-1}\mathcal{H}(\mathcal{R}\mathbf{k})\mathcal{U}. \end{aligned} \quad (9)$$

After this series of unitary transformations, wave functions of edge modes on the new edges now take the same form, which enables us to treat them on the same footing and thus to derive an effective edge Hamiltonian under the same basis. In exchange, we are left with a bulk Hamiltonian relating to original Hamiltonian through certain transformations detailed in Eq.(9), which take distinct forms across the new edges. Next, we shall project these bulk Hamiltonian which vary across edges onto a fixed edge space spanned by $\{\Psi_{\uparrow}^{BC}, \Psi_{\downarrow}^{BC}\}^T$ given by Eq.(6). Eventually, we arrive at the effective edge Hamiltonian in the 1D system, which reads

$$\mathcal{H}_{1D}^{Edge} = -\Delta k_x \eta_z - V \sin(\theta + \phi + 2\varphi_n) \eta_y, \quad (10)$$

with φ_n being the same as in Eq.(7). Eq.(10) now describes a massless spinor field in 1D space subject to a spatially varying mass field. Note that the mass terms in Eq.(10) are exactly the same as those appearing in Eq.(7). This is because the basis we chose in deriving Hamiltonian (7) happens to satisfy the relation in Eq.(8), and as a consequence the unitary transformation for Hamiltonian in Eq.(9) and that for edge basis exactly cancels with each other when projecting the Zeeman field onto the new edge space. Since the edge Hamiltonian (10) was written in the same basis, the mass term could now be used to identify relative signs of edge gaps for any two edges. From Eq.(10) it follows that the mass profile varies across the edges, and a kink is supposed to form at the corner where the mass term reverses sign, accompanied by the emergence of nontrivial MZMs protected by particle-hole symmetry, as have been well established in the seminal paper by Jackiw and Rebbi[41]. In the insets of Fig.3, we plotted the mass profile given by Eq.(10) for the 1D system, which apparently demonstrates that, whenever a kink forms at certain corner there would be one single MZM localized around. The decaying length for these MCSs along the two intersecting edges is inversely proportional to the mass term of each edge. Since the mass field is a sine function of the orientation θ of the in-plane Zeeman field, kinks and MCSs accompanied with them could thus be driven across edges and hop from one corner to a neighboring one, as we have already seen in Fig. 3(a)-(d). After the field rotates by 2π , the mass field reverts to its original configuration, during which MCSs exactly make a full circle along the boundary.

We further notice that, following from the effective Hamiltonian in Eq.(10), mass terms for opposite edges always manifest reverse signs, whatever θ and ϕ take. This is because two consecutive C_4 rotation or a C_2 rotation of bulk Hamiltonian, like the one in $DA \rightarrow D'A'$ from Eq.(9), sends (σ_x, σ_y) to $(-\sigma_x, -\sigma_y)$, thus being

equivalent to reversing the orientation of in-plane Zeeman fields. In other words, the Zeeman-field induced mass terms are odd under C_2 rotation. Therefore, if all the four edges are gapped out by the field, one can verify that there would always be two corners where adjacent edges with opposite masses intersect. Moreover, the two corners reside on the same diagonal of the lattice, each of which supports one single MZM, as shown in Fig.3 (a) and (c). Also note that, σ_x and σ_y term both preserve the inversion symmetry \mathcal{I} (differing with C_2 rotation by a unitary transformation $\tau_z \sigma_z$) as we have established in Eq.(4). Consequently, the distribution of MZMs also preserves inversion symmetry as shown in Fig.3 (a)-(d).

Interestingly, one may verify that σ_x , σ_y and τ_y are the only three \mathbf{k} -independent terms that could gap out the edges of a $p \pm ip$ superconductor. Contrary to σ_x and σ_y term, a perturbation like $\Delta_s \tau_y$ is even under C_2 rotation and meanwhile breaks inversion symmetry \mathcal{I} . We can expect it to introduce a mass term being the same on opposite edges. Indeed, upon projecting this τ_y term onto edge space, we find it gives rise to an additional mass term given by $-\Delta_s \eta_y$, independent of the edges. Again, we compare this mass term derived in a cylinder geometry with numerical results obtained for a finite lattice, which agrees well as shown in Fig.2(b). Since τ_y term only leads to a global shift of mass profile in Hamiltonian (10), kinks in the mass profile could then survive provided the perturbation is weak enough comparing to the Zeeman field. As a result, MCSs continue to exist as can be found in Fig. 2(b) and Fig. 3(e)-(h). However, the distribution of MZMs no longer preserves inversion symmetry \mathcal{I} . Increasing τ_y term further would eliminate the kinks and drives the system into a trivial phase.

V. DISCUSSION AND CONCLUSION

A $p \pm ip$ superconductor is the simplest model of time-reversal-invariant TSCs in 2D. In Ref.[38], Zhang *et al.* introduced a Rashba semiconductor/nodeless iron-based superconductor heterostructure as a promising platform to realize a 2D TSC protected by TRS. Similar to the $p \pm ip$ superconductor, we consider applying an in-plane Zeeman field $\mathbf{V} = (V \cos \theta, V \sin \theta, 0)$ to this system, and find that MZMs could also occur at corners, as is shown in Fig. 5. Furthermore, just like in a $p \pm ip$ superconductor, rotating the magnetic field in the plane would also move MCSs among the four corners.

Other promising candidates for time-reversal-invariant TSC in 2D include Rashba bilayer with interlayer interactions[42], Rashba semiconductor with two bands differing by a π -phase shift in s -wave superconducting order parameter[43], and some other interesting systems[44–46]. The low energy theory for them could all be described by a $p \pm ip$ superconductor. An in-plane magnetic field applied in these systems, however, may take distinct forms when projected to the low energy theory, and thus may or may not gap out the edges. It would

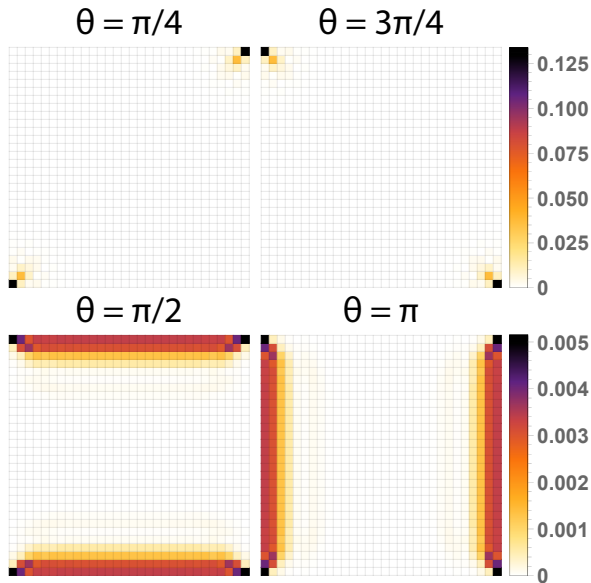


FIG. 5. Probability density plot of MZMs for a 30×30 lattice introduced in Ref.[38] with an additional in-plane magnetic field applied. Parameters in the lattice Hamiltonian therein are chosen to be, $t = 1$, $\lambda_R = 1$, $\mu = -1$, $\Delta_0 = -\Delta_1 = -2$. Strength of the Zeeman field $V = 1$.

be interesting to inspect these specific systems and see if an in-plane magnetic field could give rise to MCSs.

In conclusion, we demonstrate that a 2D $p \pm ip$ superconductor protected by TRS could support MCSs when an in-plane magnetic field is applied. By mapping all the four edges onto a 1D system, we identified the relative signs of Zeeman-field-induced masses among the four edges. MZMs form at the intersection of two adjacent edges when the mass flips sign between the two edges. Two MCSs that separate from each other in space could be induced in this model, and the positions of them could be tuned simply by rotating the in-plane magnetic field. When the field rotates by 2π , each MCS confined on the boundary would make a full circle around the system center accordingly. The simplicity manifested while tuning MCSs makes the system a potential platform to perform braidings of MZMs[47].

Note added. Recently we became aware of related work in Refs.[48,49].

ACKNOWLEDGMENTS

I would like to thank W. Chen for many stimulating discussions. This work was supported by National Science Foundation of China under Grant No. 11704305.

[1] E. Majorana, *Il Nuovo Cimento (1924-1942)* **14**, 171 (1937).
[2] F. Wilczek, *Nat Phys* **5**, 614 (2009).
[3] N. Read and D. Green, *Phys. Rev. B* **61**, 10267 (2000).
[4] A. Y. Kitaev, *Physics-Uspekhi* **44**, 131 (2001).
[5] L. Fu and C. L. Kane, *Phys. Rev. Lett.* **100**, 096407 (2008).
[6] R. M. Lutchyn, J. D. Sau, and S. Das Sarma, *Phys. Rev. Lett.* **105**, 077001 (2010).
[7] Y. Oreg, G. Refael, and F. von Oppen, *Phys. Rev. Lett.* **105**, 177002 (2010).
[8] J. Alicea, *Reports on Progress in Physics* **75**, 076501 (2012).
[9] S. R. Elliott and M. Franz, *Rev. Mod. Phys.* **87**, 137 (2015).
[10] C. W. J. Beenakker, *Annual Review of Condensed Matter Physics* **4**, 113 (2013).
[11] T. D. Stanescu and S. Tewari, *Journal of Physics: Condensed Matter* **25**, 233201 (2013).
[12] V. Mourik, K. Zuo, S. M. Frolov, S. R. Plissard, E. P. A. M. Bakkers, and L. P. Kouwenhoven, *Science* **336**, 1003 (2012).
[13] A. Das, Y. Ronen, Y. Most, Y. Oreg, M. Heiblum, and H. Shtrikman, *Nat Phys* **8**, 887 (2012).
[14] M. T. Deng, C. L. Yu, G. Y. Huang, M. Larsson, P. Caroff, and H. Q. Xu, *Nano Letters* **12**, 6414 (2012).
[15] L. P. Rokhinson, X. Liu, and J. K. Furdyna, *Nat Phys* **8**, 795 (2012).
[16] A. D. K. Finck, D. J. Van Harlingen, P. K. Mohseni, K. Jung, and X. Li, *Phys. Rev. Lett.* **110**, 126406 (2013).
[17] S. Nadj-Perge, I. K. Drozdov, J. Li, H. Chen, S. Jeon, J. Seo, A. H. MacDonald, B. A. Bernevig, and A. Yazdani, *Science* **346**, 602 (2014).
[18] M. T. Deng, S. Vaitiekėnas, E. B. Hansen, J. Danon, M. Leijnse, K. Flensberg, J. Nygård, P. Krogstrup, and C. M. Marcus, *Science* **354**, 1557 (2016).
[19] J.-P. Xu, M.-X. Wang, Z. L. Liu, J.-F. Ge, X. Yang, C. Liu, Z. A. Xu, D. Guan, C. L. Gao, D. Qian, Y. Liu, Q.-H. Wang, F.-C. Zhang, Q.-K. Xue, and J.-F. Jia, *Phys. Rev. Lett.* **114**, 017001 (2015).
[20] H.-H. Sun, K.-W. Zhang, L.-H. Hu, C. Li, G.-Y. Wang, H.-Y. Ma, Z.-A. Xu, C.-L. Gao, D.-D. Guan, Y.-Y. Li, C. Liu, D. Qian, Y. Zhou, L. Fu, S.-C. Li, F.-C. Zhang, and J.-F. Jia, *Phys. Rev. Lett.* **116**, 257003 (2016).
[21] M. Sitte, A. Rosch, E. Altman, and L. Fritz, *Phys. Rev. Lett.* **108**, 126807 (2012).
[22] J. C. Y. Teo and T. L. Hughes, *Phys. Rev. Lett.* **111**, 047006 (2013).
[23] F. Zhang, C. L. Kane, and E. J. Mele, *Phys. Rev. Lett.* **110**, 046404 (2013).
[24] W. A. Benalcazar, J. C. Y. Teo, and T. L. Hughes, *Phys. Rev. B* **89**, 224503 (2014).
[25] W. A. Benalcazar, B. A. Bernevig, and T. L. Hughes, *Science* **357**, 61 (2017).
[26] W. A. Benalcazar, B. A. Bernevig, and T. L. Hughes, *Phys. Rev. B* **96**, 245115 (2017).
[27] F. Schindler, A. M. Cook, M. G. Vergniory, Z. Wang, S. S. P. Parkin, B. A. Bernevig, and T. Neupert, arXiv:1708.03636.

- [28] J. Langbehn, Y. Peng, L. Trifunovic, F. von Oppen, and P. W. Brouwer, Phys. Rev. Lett. **119**, 246401 (2017).
- [29] Z. Song, Z. Fang, and C. Fang, Phys. Rev. Lett. **119**, 246402 (2017).
- [30] S. Imhof, C. Berger, F. Bayer, J. Brehm, L. Molenkamp, T. Kiessling, F. Schindler, C. H. Lee, M. Greiter, T. Neupert, and R. Thomale, arXiv:1708.03647.
- [31] C. W. Peterson, W. A. Benalcazar, T. L. Hughes, and G. Bahl, arXiv:1710.03231.
- [32] F. K. Kunst, G. van Miert, and E. J. Bergholtz, arXiv:1712.07911.
- [33] M. Ezawa, Phys. Rev. Lett. **120**, 026801 (2018).
- [34] M. Serra-Garcia, V. Peri, R. Süssstrunk, O. R. Bilal, T. Larsen, L. G. Villanueva, and S. D. Huber, Nature (2018).
- [35] G. E. Volovik, JETP Letters **91**, 201 (2010).
- [36] A. P. Schnyder, S. Ryu, A. Furusaki, and A. W. W. Ludwig, Phys. Rev. B **78**, 195125 (2008).
- [37] C.-K. Chiu, J. C. Y. Teo, A. P. Schnyder, and S. Ryu, Rev. Mod. Phys. **88**, 035005 (2016).
- [38] F. Zhang, C. L. Kane, and E. J. Mele, Phys. Rev. Lett. **111**, 056402 (2013).
- [39] X.-L. Qi, T. L. Hughes, S. Raghu, and S.-C. Zhang, Phys. Rev. Lett. **102**, 187001 (2009).
- [40] X.-L. Qi and S.-C. Zhang, Rev. Mod. Phys. **83**, 1057 (2011).
- [41] R. Jackiw and C. Rebbi, Phys. Rev. D **13**, 3398 (1976).
- [42] S. Nakosai, Y. Tanaka, and N. Nagaosa, Phys. Rev. Lett. **108**, 147003 (2012).
- [43] S. Deng, L. Viola, and G. Ortiz, Phys. Rev. Lett. **108**, 036803 (2012).
- [44] J. Wang, Y. Xu, and S.-C. Zhang, Phys. Rev. B **90**, 054503 (2014).
- [45] F. Yang, C.-C. Liu, Y.-Z. Zhang, Y. Yao, and D.-H. Lee, Phys. Rev. B **91**, 134514 (2015).
- [46] J. M. Midtgård, Z. Wu, and G. M. Bruun, Phys. Rev. A **96**, 033605 (2017).
- [47] C. Nayak, S. H. Simon, A. Stern, M. Freedman, and S. Das Sarma, Rev. Mod. Phys. **80**, 1083 (2008).
- [48] E. Khalaf, arXiv:1801.10050.
- [49] M. Geier, L. Trifunovic, M. Hoskam, and P. W. Brouwer, arXiv:1801.10053.